



# Bismuth-Catalyzed Amide Reduction

**DOI:**

[10.1002/anie.202306447](https://doi.org/10.1002/anie.202306447)

**Document Version**

Final published version

[Link to publication record in Manchester Research Explorer](#)

**Citation for published version (APA):**

Yang, X., Kuziola, J., Béland, V. A., Busch, J., Leutzsch, M., Burés, J., & Cornella, J. (2023). Bismuth-Catalyzed Amide Reduction. *Angewandte Chemie International Edition*. <https://doi.org/10.1002/anie.202306447>

**Published in:**

Angewandte Chemie International Edition

**Citing this paper**

Please note that where the full-text provided on Manchester Research Explorer is the Author Accepted Manuscript or Proof version this may differ from the final Published version. If citing, it is advised that you check and use the publisher's definitive version.

**General rights**

Copyright and moral rights for the publications made accessible in the Research Explorer are retained by the authors and/or other copyright owners and it is a condition of accessing publications that users recognise and abide by the legal requirements associated with these rights.

**Takedown policy**

If you believe that this document breaches copyright please refer to the University of Manchester's Takedown Procedures [<http://man.ac.uk/04Y6Bo>] or contact [uml.scholarlycommunications@manchester.ac.uk](mailto:uml.scholarlycommunications@manchester.ac.uk) providing relevant details, so we can investigate your claim.



**Homogeneous Catalysis**
**Bismuth-Catalyzed Amide Reduction**

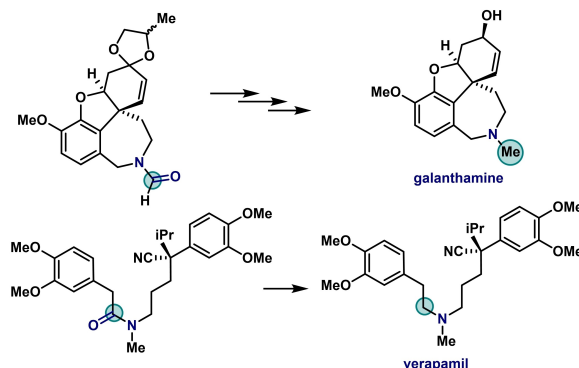
 Xiuxiu Yang, Jennifer Kuziola<sup>+</sup>, Vanessa A. Béland<sup>+</sup>, Julia Busch, Markus Leutzsch, Jordi Burés,<sup>\*</sup> and Josep Cornella<sup>\*</sup>

**Abstract:** In this article we report that a cationic version of Akiba's Bi<sup>III</sup> complex catalyzes the reduction of amides to amines using silane as hydride donor. The catalytic system features low catalyst loadings and mild conditions, en route to secondary and tertiary aryl- and alkylamines. The system tolerates functional groups such as alkene, ester, nitrile, furan and thiophene. Kinetic studies on the reaction mechanism result in the identification of a reaction network with an important product inhibition that is in agreement with the experimental reaction profiles.

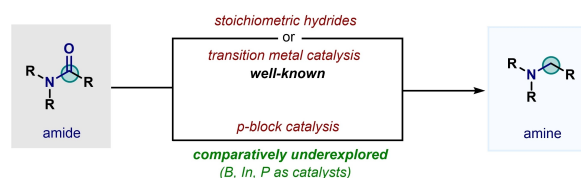
The non-toxicity associated to certain bismuth (Bi) salts<sup>[1]</sup> has led to an increasing number of reports studying their potential applications, in particular, in the context of synthetic chemistry.<sup>[2]</sup> Whereas examples exploiting Bi's catalytic redox properties have only recently emerged,<sup>[2c,d,f,g]</sup> organic transformations capitalizing on the Lewis acidity of Bi<sup>III</sup> compounds are well-known and studied.<sup>[3]</sup> The acidity of bismuth is strongly related to the relativistic effects: lowering the energies of frontier 6s and 6p orbitals is crucial for the efficient coordination and further catalysis. Despite the numerous examples based on this concept,<sup>[3]</sup> hydrogenation/reduction reactions are largely underexplored.<sup>[2c,4]</sup> An efficient transfer hydrogenation of azo- and nitroarenes from ammonia borane/H<sub>2</sub>O was realized by mononuclear Bi<sup>I</sup> species supported by a *N,C,N* pincer ligand.<sup>[2c]</sup> The strong Lewis acidity of a cationic Bi<sup>III</sup> complex reported by Venugopal et al. has also recently been shown to efficiently catalyze the hydrosilylation of olefins, aldehydes and ketones.<sup>[4a]</sup> It was postulated that the cationic Bi<sup>III</sup> species

can engage in the activation of Si–H bonds or the carbonyl group depending on the conditions.<sup>[4b]</sup> We envisaged that the interesting Lewis acidic properties of cationic Bi<sup>III</sup> complexes would also be beneficial in the activation of more challenging compounds such as amides, en route to valuable amines. Amide bond formation is one of the most utilized reactions in the synthetic chemistry space, and is a coveted strategy for the synthesis of amines (Scheme 1A).<sup>[5]</sup> Yet, as a result of the resonance stability of amides, reduction of amides are more challenging compared to other carbonyl compounds.<sup>[6]</sup> Although examples based on stoichiometric reducing agents (LiAlH<sub>4</sub>, DIBAL-H, Red-Al, H<sub>2</sub> gas, borane, etc.)<sup>[5]</sup> and transition metal catalysis exist (Mn, Fe, Ni, Zn, Mo, Ru, Rh, Ir, Pt, Sm),<sup>[6a,7]</sup> seldom examples are known employing *p*-block elements as catalysts.<sup>[8]</sup> Group 13 complexes based on boron and indium have indeed been

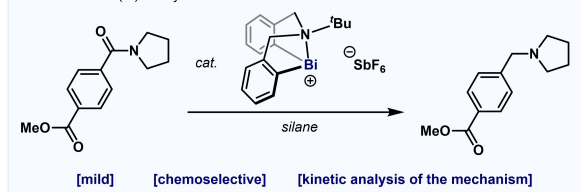
## A. Amines from amides: a relevant synthetic strategy in industrial settings



## B. Amide reduction: an overview



## C. This work: Bi(III)-catalyzed reduction of amides to amines



**Scheme 1.** A) Examples of amide reduction in pharma industries. B) Strategies for amide reduction. C) Bi-catalyzed reduction of amides.

[\*] Dr. X. Yang, J. Kuziola,<sup>+</sup> Dr. V. A. Béland,<sup>+</sup> J. Busch, Dr. M. Leutzsch, Dr. J. Cornella  
 Max-Planck-Institut für Kohlenforschung  
 Kaiser-Wilhelm-Platz 1, 45470 Mülheim an der Ruhr (Germany)  
 E-mail: cornella@kofo.mpg.de

Dr. J. Burés  
 University of Manchester  
 Oxford Road, M13 9PL Manchester (UK)  
 E-mail: jordi.bures@manchester.ac.uk

[†] These authors contributed equally to this work.

© 2023 The Authors. Angewandte Chemie International Edition published by Wiley-VCH GmbH. This is an open access article under the terms of the Creative Commons Attribution Non-Commercial NoDerivs License, which permits use and distribution in any medium, provided the original work is properly cited, the use is non-commercial and no modifications or adaptations are made.

reported;<sup>[8a-d]</sup> yet, to the best of our knowledge, a single example based on a group 15 catalyst (phosphorous) is known.<sup>[8c]</sup> Herein, we report the ability of a cationic bismuth complex in catalyzing the hydrodeoxygenation of tertiary and secondary amides, using a simple silane as H donor. The high chemoselectivity of the catalyst permits the tolerance of various functional groups, including nitriles, esters, ethers and heterocycles. Detailed kinetic studies provided orders of reaction of components and revealed that the resulting amine product inhibits reactivity. We were also able to provide a plausible reaction network capable of reproducing all our experimental observations.

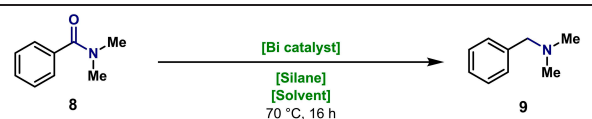
To tackle this synthetic challenge, we selected 1,1,3,3-tetramethyldisiloxane (TMDSO) as H source since it is cheap, moisture stable, neutral and has been widely explored in the reduction of functional groups.<sup>[9]</sup> Dimethyl benzamide **8** was selected as the model substrate. The use of 10 mol % Lewis-acidic Bi(OTf)<sub>3</sub> or BiCl<sub>3</sub>/AgSbF<sub>6</sub> did not lead to any reduction of **8** (Table 1, entries 1 and 2). On top of this, we screened diaryl Bi<sup>III</sup> complexes featuring supportive heteroatoms built into the ligand backbone. Akiba's complex **3**,<sup>[10]</sup> featuring a bis-benzyl N<sup>-</sup>Bu amine, gave 62 % of **9** in C<sub>6</sub>D<sub>6</sub> at 70 °C (entry 5). Sulfoximine- and sulfoxide-based Bi<sup>III</sup> catalysts (**4**, **5**, **6**, and **7**) employed in

Bi<sup>III</sup>/Bi<sup>V</sup> redox processes failed to provide **9** (entries 6–9).<sup>[2a,f,g,11]</sup> The yield of **9** was optimized to 92 % by switching to MeCN. We speculate that the coordinating ability of MeCN plays a role in this boost of reactivity, through cation stabilization. Control experiments revealed the requirement of both AgSbF<sub>6</sub> and Bi in the system (entries 13 and 14). It was found that the SbF<sub>6</sub><sup>-</sup> anion can be substituted with tetrakis(3,5-bis(trifluoromethyl)phenyl)borate (BARF)<sup>[12]</sup> or triflate (OTf) anions to give the same high optimized yield (entries 15 and 16). However, the replacement of SbF<sub>6</sub><sup>-</sup> with BF<sub>4</sub><sup>-</sup> or PF<sub>6</sub><sup>-</sup> anions completely inhibits reactivity (entries 17 and 18), which indicates the important effect of the counter-anion.<sup>[13]</sup> Importantly, 2 equiv of PhSiH<sub>3</sub> resulted in 42 % yield of **9** (entry 19 and see below).

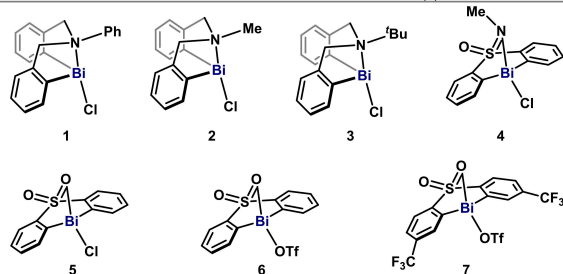
Next, we explored the generality of the reduction protocol. As shown in Scheme 2, benzamides of cyclic secondary amines (piperidine, **10**; morpholine, **11**; pyrrolidine, **12**) or acyclic (diethylamine, **13**) amines were reduced successfully under the optimized conditions. Benzamides of hexylamine and aniline (both primary amines) were also converted into the corresponding amines in good yields (**14** and **15**). Taking pyrrolidine as the model amine, the carbonyl substituent was interrogated. In this sense,  $\pi$ -extended (**16**) and *ortho*-Me substituted (**17**) were both amenable. Heterocyclic furan (**18**) and thiophene (**19**) boded well in this protocol. *para*-Substituted pyrrolidinebenzamides with halogens (F, C, Br, I, **20–23**) or CF<sub>3</sub> (**24**) were satisfactorily reduced in good yields. A silyl protected ether could also be tolerated (**25**). Sensitive functional groups amenable to reduction such as nitrile (**26**) or ester (**27**) were tolerated. Electron-releasing substituents such as alkyl or ether could be accommodated (**28–30**). Interestingly, the symmetric tris-benzamide **30** was also reduced in good yields. Alkene functionality (**32**) could be tolerated. Challenging amides derived from alkyl carboxylic acids, for example, from cyclohexyl carboxylic acid such as **33** and **34** were successfully converted to amines. Moreover, non-cyclic amides such as **35** or **36** were well accommodated. Finally, cyclic 6 and 7-membered lactams provided the cyclic amine in excellent yields (**37** and **38**). It is important to mention that no intermediate or side product was detected in these reactions, thus highlighting the high chemoselectivity of the process. Yet, the byproduct of the silane was difficult to trace and at present, we speculate is a polymeric based siloxane (see Supporting Information).

In order to gain insight into the mechanism of the transformation, we selected amide **12** and monitored the conversion to **40** under standard reaction conditions. The reaction profile showed a marked decline of rate over the course of the reaction (Figure 1a), which could be due to several reasons. One possible explanation for this behavior could be related to the different reactivity of TMDSO-derivatives detected during the reaction. We have confirmed the formation of those hydride species during the reaction by NMR (See Supporting Information). To verify if the marked decline in rate of the reaction with TMDSO was solely due to the reaction of different hydride species and to avoid additional hurdles in the kinetic analysis, we decided to switch the hydride source to PhSiH<sub>3</sub> for the kinetic

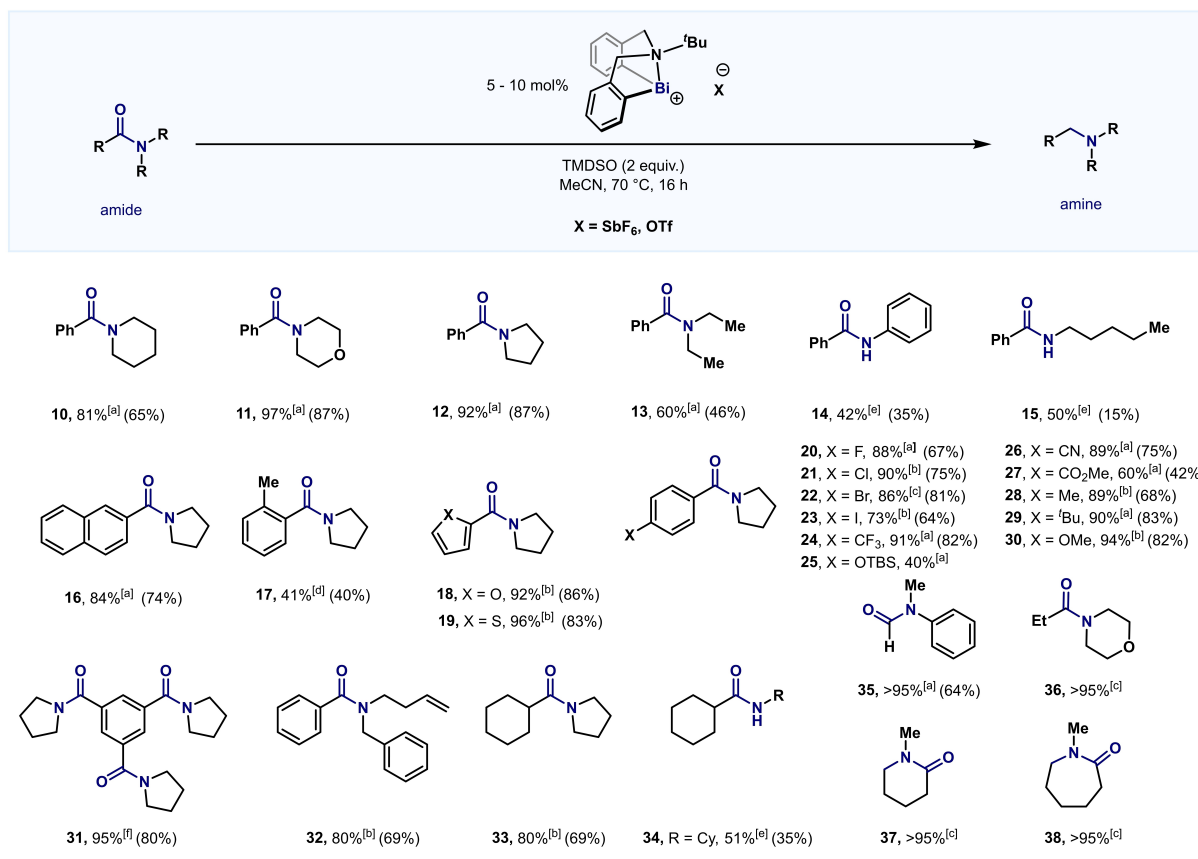
**Table 1:** Bi-catalyzed conversion of amides to amines: optimization of the reaction conditions.



entry	Bi catalyst (mol%)	solvent	silane (equiv)	yield ( <b>9</b> ) <sup>[a]</sup>
1	BiCl <sub>3</sub> /AgSbF <sub>6</sub> (10 mol%)	C <sub>6</sub> D <sub>6</sub>	TMDSO (5)	<5%
2	Bi(OTf) <sub>3</sub> (10 mol%)	C <sub>6</sub> D <sub>6</sub>	TMDSO (5)	<5%
3	<b>1</b> / AgSbF <sub>6</sub> (10 mol%)	C <sub>6</sub> D <sub>6</sub>	TMDSO (5)	<5%
4	<b>2</b> / AgSbF <sub>6</sub> (10 mol%)	C <sub>6</sub> D <sub>6</sub>	TMDSO (5)	<5%
5	<b>3</b> / AgSbF <sub>6</sub> (10 mol%)	C <sub>6</sub> D <sub>6</sub>	TMDSO (5)	62%
6	<b>4</b> / AgSbF <sub>6</sub> (10 mol%)	PhH	TMDSO (5)	<5% <sup>[b]</sup>
7	<b>5</b> / AgSbF <sub>6</sub> (10 mol%)	C <sub>6</sub> D <sub>6</sub>	TMDSO (5)	<5%
8	<b>6</b> (10 mol%)	C <sub>6</sub> D <sub>6</sub>	TMDSO (5)	<5%
9	<b>7</b> (10 mol%)	C <sub>6</sub> D <sub>6</sub>	TMDSO (5)	<5%
10	<b>3</b> / AgSbF <sub>6</sub> (10 mol%)	C <sub>6</sub> D <sub>6</sub>	TMDSO (2)	41%
11	<b>3</b> / AgSbF <sub>6</sub> (2.5 mol%)	MeCN	TMDSO (2)	59 ± 4% <sup>[c]</sup>
12	<b>3</b> / AgSbF <sub>6</sub> (5 mol%)	MeCN	TMDSO (2)	92 ± 2% <sup>[c]</sup> (85%) <sup>[d]</sup>
13	<b>3</b> (10 mol%)	MeCN	TMDSO (5)	<5%
14	AgSbF <sub>6</sub> (10 mol%)	MeCN	TMDSO (5)	<5%
15	<b>3</b> / AgOTf (5 mol%)	MeCN	TMDSO (2)	95 ± 4% <sup>[c]</sup>
16	<b>3</b> / AgBARF (5 mol%)	MeCN	TMDSO (2)	90%
17	<b>3</b> / AgBF <sub>4</sub> (5 mol%)	MeCN	TMDSO (2)	<5%
18	<b>3</b> / AgPF <sub>6</sub> (5 mol%)	MeCN	TMDSO (2)	<5%
19	<b>3</b> / AgSbF <sub>6</sub> (5 mol%)	MeCN	PhSiH <sub>3</sub> (2)	42%
20	<b>3</b> / AgSbF <sub>6</sub> (5 mol%)	MeCN	TMDSO (1)	58%



[a] Determined by integration relative to 1,3,5-trimethoxybenzene internal standard. Detailed procedure can be found in the Supporting Information. [b] Determined by integrations of amine/(amide + amine) in the <sup>1</sup>H NMR spectra. [c] Error values determined through quadruple experiments. [d] Isolated yield.



**Scheme 2.** Catalytic amide reduction. [a] [Bi/SbF<sub>6</sub>] 5 mol%, 70 °C, 20 h. [b] [Bi/OTf] 5 mol%, 70 °C, 20 h. [c] [Bi/SbF<sub>6</sub>] 10 mol%, 70 °C, 16 h. [d] [Bi/SbF<sub>6</sub>] 5 mol%, 100 °C, 20 h. [e] 1.2 equiv HBpin, heated with amide at 70 °C for 2 h, then add [Bi/SbF<sub>6</sub>] 5 mol% and silane and heat to 70 °C, 20 h. [f] [Bi/SbF<sub>6</sub>] 15 mol%, 70 °C, 20 h. Yields were calculated by quantitative <sup>1</sup>H NMR using 1,3,5-trimethoxybenzene as internal standard, while those in brackets are isolated yields.

studies. PhSiH<sub>3</sub> is a well-behaved hydride source that did not form any NMR-detectable hydride intermediate species and transferred two hydrides per molecule, as proven by the reaction stopping at 66 % yield when using 0.66 equivalents of PhSiH<sub>3</sub> (Figure 1b). Despite the absence of hydride intermediates, reactions with excess of PhSiH<sub>3</sub> also had a marked decline of rate during the course of the reaction (Figure 1c, blue circles). Another possible reason for this kinetic behavior could be the deactivation of the catalyst, for example, through the reduction of the Bi–C bond by silanes.<sup>[14]</sup> To investigate the possibility of catalyst deactivation, we performed some excess experiments (Figure 1c, green squares). Indeed, this reaction was much quicker than the standard reaction (Figure 1c, blue circles), which indicates catalyst deactivation or product inhibition. To discern between these two possibilities, we ran a same-excess reaction with product added. The overlap between the reaction profile of the standard reaction (Figure 1c, blue circles) and the time-shifted reaction profile of the same-excess reaction with product added (Figure 1c, red diamonds) demonstrates the absence of significant catalyst deactivation and evidences an important inhibition of the catalyst by the product of the reaction. This is likely due to

the stronger coordination ability of the amine compared to the amide for Bi<sup>III</sup> complexes.<sup>[15]</sup>

When we reduced (Figure 1d, red diamonds) or increased (Figure 1d, green squares) the concentration of PhSiH<sub>3</sub> with respect to the standard reaction (Figure 1d, blue circles), the initial rates of the reaction slightly increased, but the conversion after 10 h of reaction was not significantly affected. The nonlinear dependency of the rate of the reaction with respect to the concentration of PhSiH<sub>3</sub> suggests a complex reaction mechanism.

To test if higher concentrations of amide could mitigate the inhibition of the catalyst by the product, we ran three experiments with different initial concentration of amide (Figure 1e). Reactions with higher initial concentrations of amide **12** (Figure 1e, green squares) maintained the quicker kinetic regime during more turnovers since higher concentrations of product were required to outcompete the coordination of the starting material to the catalyst.

Using variable time normalization analysis (VTNA),<sup>[16]</sup> we have estimated a positive partial order in amide **12** of around 0.4 (Figure 1f) at the beginning of the reaction, where the effect of the product (**40**) on the rate of the reaction is negligible ([**40**] < 0.04 M). The partial order is consistent with a mechanism including a reversible coordina-

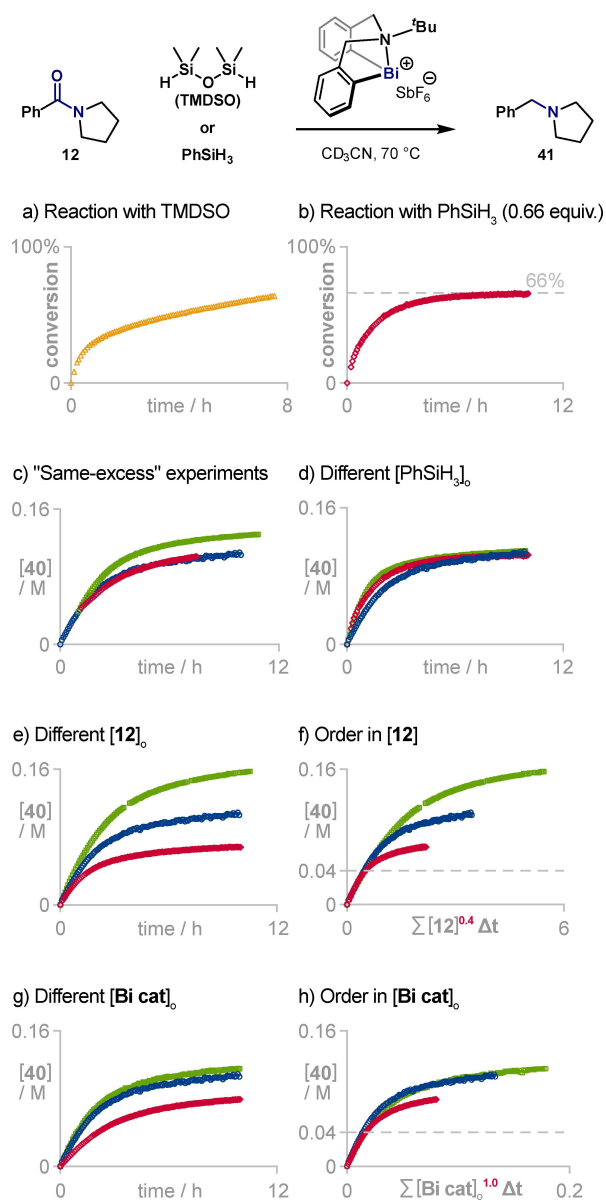


**Figure 1.** Kinetic data for the Bi-catalyzed reduction of amides. Figure 1a and 1b show conversion as  $[40]/([12] + [40]) \cdot 100$  in the y-axis. All reaction conditions and initial concentrations can be found in the Supporting Information.

tion of the amide to the catalyst under the reaction conditions.

We also investigated the effect of the concentration of catalyst on the rate of the reaction (Figure 1g). As in the case of the amide, we have analyzed the beginning of the reaction profiles ( $[P] < 0.04$  M) to minimize the interference of the product inhibition in the rate of the reaction. The analysis of the normalized-time scale<sup>[16]</sup> reaction profiles of three reactions with different initial concentration of catalyst revealed a standard order 1 in catalyst (Figure 1h). This is consistent with a mechanism that does not involve significant amounts of neither active nor inactive dimeric or higher order bismuth species.

To investigate the mechanism of the reaction further we have used kinetic modelling software to explore the fitting of the experimental kinetic data to several kinetic models shown in Figure 2 (see Supporting Information). In total, we have used seven reaction profiles for the fitting: the profiles for the standard reaction and for reactions with higher and lower initial concentrations of  $\text{PhSiH}_3$ , amide **12** or Bi catalyst than the standard reaction. Fitting all reaction profiles is very challenging for most of the models due to the intrinsic complexity of each profile, and the diversity of initial reaction conditions explored among all seven experiments. Indeed, mechanisms involving catalytic species of bismuth only able to coordinate one molecule of amide, hydride or product at a time are insufficient to capture the full mechanistic complexity of the system (**M1–M4**, see Supporting Information). However, **M5**, which contains catalytic species with up to two silanes, amides or amines coordinated to the same bismuth catalyst is flexible enough to fit all the experimental data reasonably well. This is not unreasonable given the dramatic influence of the coordinating pendant amine in reactivity and the ability of cationic diarylbismuth(III) complexes for hypervalent 3c–4e bonding in the *p* orbital.<sup>[3c,17]</sup> Importantly, **M5** predicts with high accuracy the kinetics of the same-excess experiment even though its profile was not used in the original fitting. Also, it is remarkable that **M5** reproduces the unexpected changes on kinetic regimes occurring at different conversions for different catalyst loadings, despite not containing dimeric bismuth catalytic species, nor catalyst deactivation steps.

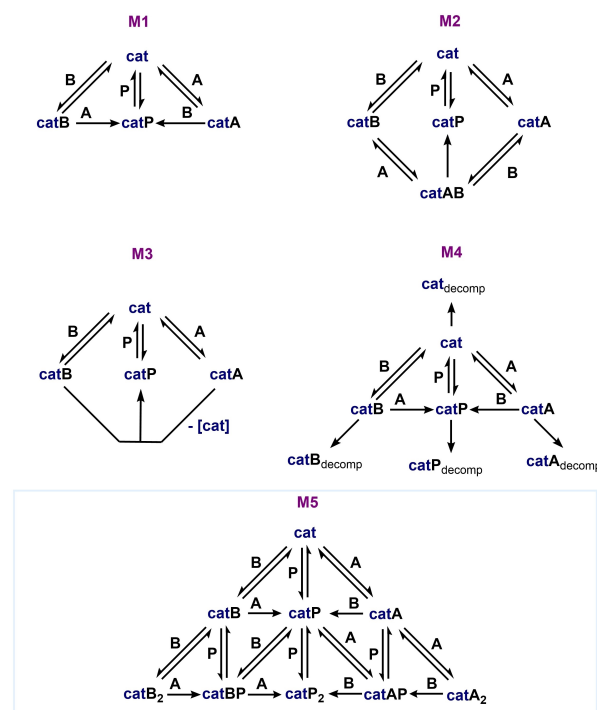


**Figure 2.** Selection of 5 kinetic models considered for the fitting of the experimental data. A: amide; B:  $\text{PhSiH}_3$ ; cat: catalyst. See Supporting Information for the complete list of models considered and fittings.

In conclusion, we have developed a protocol for the reduction of amides using a cationic Bi<sup>III</sup> precursor as catalyst. The protocol is characterized by the compatibility of Bi<sup>III</sup> with a silane, which allows the reduction of >25 aliphatic and aromatic amides. In this manner, a variety of tertiary and secondary amines can be obtained in good to excellent yields. Mechanistic studies on a model reaction using PhSiH<sub>3</sub> revealed that at the initial stages, the reaction is order one in Bi, which suggests monomeric species being dominant. It was found that at high concentrations of amine, the reaction became slower due to competing coordination at the Bi center, thus ruling out possible catalyst decomposition pathways. Finally, a putative reaction network that enables the catalyst to engage with two components satisfactorily reproduces the experimental data. More importantly, the kinetic model **M5** is also able to predict kinetic behavior which was not used as a source of data to generate it. This protocol represents one of the first attempts to elucidate catalytic mechanisms based on Bi using VTNA.<sup>[17]</sup>

### Acknowledgements

Financial support for this work was provided by Max-Planck-Gesellschaft, Max-Planck-Institut für Kohlenforschung, Fonds der Chemischen Industrie (FCI-VCI), Natural Sciences and Engineering Council of Canada (NSERC: PDF-558027-2021) and The University of Manchester. This project received funding from the European Research Council (ERC Starting Grant No. 850496 to J.C.). We specially thank the analytical departments (Xray, NMR) and Prof. Dr. A. Fürstner for generous support. Open Access funding enabled and organized by Projekt DEAL.

### Conflict of Interest

The authors declare no conflict of interest.

### Data Availability Statement

The data that support the findings of this study are available in the Supporting Information of this article.

**Keywords:** Amides · Bismuth · Kinetics · Reaction Mechanisms · Reduction

- [1] a) R. Mohan, *Nat. Chem.* **2010**, *2*, 336–336; b) P. de Marcillac, N. Coron, G. Dambier, J. Leblanc, J.-P. Moalic, *Nature* **2003**, *422*, 876–878.  
[2] a) O. Planas, F. Wang, M. Leutzsch, J. Cornella, *Science* **2020**, *367*, 313–317; b) M. Magre, J. Cornella, *J. Am. Chem. Soc.* **2021**, *143*, 21497–21502; c) F. Wang, O. Planas, J. Cornella, *J. Am. Chem. Soc.* **2019**, *141*, 4235–4240; d) Y. Pang, M. Leutzsch, N. Nöthling, J. Cornella, *J. Am. Chem. Soc.* **2020**, *142*, 19473–19479; e) M. Jurrat, L. Maggi, W. Lewis, L. T. Ball, *Nat. Chem.*

- 2020**, *12*, 260–269; f) O. Planas, V. Peciukenas, J. Cornella, *J. Am. Chem. Soc.* **2020**, *142*, 11382–11387; g) O. Planas, V. Peciukenas, M. Leutzsch, N. Nöthling, D. A. Pantazis, J. Cornella, *J. Am. Chem. Soc.* **2022**, *144*, 14489–14504.  
[3] a) T. Ollevier, *Org. Biomol. Chem.* **2013**, *11*, 2740–2755; b) E. Lopez, S. C. Thorp, R. S. Mohan, *Polyhedron* **2022**, *222*, 115765; c) C. Lichtenberg, *Chem. Commun.* **2021**, *57*, 4483–4495; d) J. Ramler, K. Hofmann, C. Lichtenberg, *Inorg. Chem.* **2020**, *59*, 3367–3376; e) J. M. Bothwell, S. W. Krabbe, R. S. Mohan, *Chem. Soc. Rev.* **2011**, *40*, 4649–4707; f) A. Gagnon, J. Dansereau, A. Le Roch, *Synthesis* **2017**, *49*, 1707–1745.  
[4] a) S. Balasubramaniam, S. Kumar, A. P. Andrews, B. Varghese, E. D. Jemmis, A. Venugopal, *Eur. J. Inorg. Chem.* **2019**, 3265–3269; b) R. Kannan, S. Balasubramaniam, S. Kumar, R. Chammenahalli, E. D. Jemmis, A. Venugopal, *Chem. Eur. J.* **2020**, *26*, 12717–12721.  
[5] J. Magano, J. R. Dunetz, *Org. Process Res. Dev.* **2012**, *16*, 1156–1184.  
[6] a) A. Volkov, F. Tinnis, T. Slagbrand, P. Trillo, H. Adolfsson, *Chem. Soc. Rev.* **2016**, *45*, 6685–6697; b) D. Addis, S. Das, K. Junge, M. Beller, *Angew. Chem. Int. Ed.* **2011**, *50*, 6004–6011.  
[7] A. Chardon, E. Morisset, J. Rouden, J. Blanchet, *Synthesis* **2018**, *50*, 984–997.  
[8] a) N. Sakai, K. Fujii, T. Konakahara, *Tetrahedron Lett.* **2008**, *49*, 6873–6875; b) Y. Li, J. A. Molina de La Torre, K. Grabow, U. Bentrup, K. Junge, S. Zhou, A. Brückner, M. Beller, *Angew. Chem. Int. Ed.* **2013**, *52*, 11577–11580; c) M.-C. Fu, R. Shang, W.-M. Cheng, Y. Fu, *Angew. Chem. Int. Ed.* **2015**, *54*, 9042–9046; d) D. Mukherjee, S. Shirase, K. Mashima, J. Okuda, *Angew. Chem. Int. Ed.* **2016**, *55*, 13326–13329; e) A. Augurusa, M. Mehta, M. Perez, J. Zhu, D. W. Stephan, *Chem. Commun.* **2016**, *52*, 12195–12198.  
[9] J. Pesti, G. L. Larson, *Org. Process Res. Dev.* **2016**, *20*, 1164–1181.  
[10] a) K. Ohkata, M. Ohnishi, K.-y. Akiba, *Tetrahedron Lett.* **1988**, *29*, 5401–5404; b) M. Bao, T. Hayashi, S. Shimada, *Organometallics* **2007**, *26*, 1816–1822.  
[11] H. W. Moon, J. Cornella, *ACS Catal.* **2022**, *12*, 1382–1393.  
[12] S. H. Strauss, *Chem. Rev.* **1993**, *93*, 927–942.  
[13] We encountered severe fluctuations in yields when aged AgSbF<sub>6</sub> was used, probably due to fluoride-containing by-products inhibiting salt metathesis and cation reactivity. See T. Dunaj, J. Schwarzmann, J. Ramler, A. Stoy, S. Reith, J. Nitzche, L. Völlinger, C. von Hänisch, C. Lichtenberg, *Chem. Eur. J.* **2023**, *29*, e202204012. Further details about this aspect can be found in the Supporting Information.  
[14] Y. Pang, M. Leutzsch, N. Nöthling, F. Katzenburg, J. Cornella, *J. Am. Chem. Soc.* **2021**, *143*, 12487–12493.  
[15] a) G. G. Briand, N. Burford, *Advances in Inorganic Chemistry*, Vol. 50, Academic Press, New York, **2000**, pp. 285–357; b) T. J. Boyle, D. M. Pedrotty, B. Scott, J. W. Zillere, *Polyhedron* **1998**, *17*, 1959–1974; c) G. G. Briand, N. Burford, T. S. Cameron, W. Kwiatkowski, *J. Am. Chem. Soc.* **1998**, *120*, 11374–11379.  
[16] a) J. Burés, *Angew. Chem. Int. Ed.* **2016**, *55*, 16084; b) D.-T. C. Nielsen, J. Burés, *Chem. Sci.* **2019**, *10*, 348.  
[17] During the revision of this manuscript, a mechanistic work on Bi-catalyzed reduction of ketones appeared in the peer-reviewed literature: A. Benny, D. Sharma, Ankur, T. Rajeshkumar, L. Maron, A. Venugopal, *Chem. Eur. J.* **2023**, *29*, e202300588, *accepted article*.

Manuscript received: May 8, 2023

Accepted manuscript online: June 7, 2023

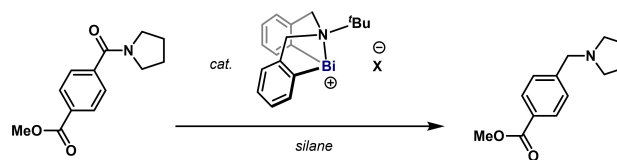
Version of record online: ■■■, ■■■

## Communications

## Homogeneous Catalysis

X. Yang, J. Kuziola, V. A. Béland, J. Busch,  
M. Leutzsch, J. Burés,\*  
J. Cornella\* [e202306447](#)

## Bismuth-Catalyzed Amide Reduction



[mild]

[chemoselective]

[kinetic analysis]

[&gt;25 examples]

We report a protocol for the reduction of amides to amines using a cationic Bi<sup>III</sup> catalyst with a tridentate ligand framework in combination with a simple and cheap silane as the reducing agent. Various amides can be reduced and a

variety of functional groups can be tolerated. Kinetic analyses and modeling were used to elucidate the orders of each component and to generate a kinetic model that is in agreement with the observed experimental data.